

Microstructure and in Vitro Corrosion Properties of ZK60 Magnesium Alloy Coated with Calcium Phosphate by Electrodeposition at Different Temperatures

Wei Lu^{1,*,**}, Caiwen Ou^{2,**}, Zailei Zhan¹, Ping Huang¹, Biao Yan¹ and Minsheng Chen^{2,*}

¹ School of Materials Science and Engineering, Shanghai Key Lab. of D&A for Metal-Functional Materials, Tongji University, Shanghai 200092, China

² Southern Medical University, No.1023, Shatai Nan Road, Guangzhou City, Guangzhou 510515, China

*E-mail: weilu@tongji.edu.cn; gzminsheng@vip.163.com

** These authors made equal contributions to this work.

Received: 26 May 2013 / Accepted: 6 July 2013 / Published: 1 August 2013

Magnesium and its alloys have attracted more and more attentions due to their potential applications in biodegradable implants. But the applications are limited by high corrosion rate of magnesium. In this paper, CaP coatings were fabricated on the ZK60 magnesium alloys by a electrodeposition method. The coatings were composed of mainly DCPD phases with flake-like structure. SEM images show that the particle size and surface roughness in the coatings increase with increasing electrolyte temperatures. Electrochemical corrosion and in vitro immersion were conducted to evaluate the corrosion resistance. The corrosion resistance of the coated samples was greatly improved comparing with that of the uncoated sample. For the samples fabricated at different electrolyte temperatures, the sample coated at 60 °C has the best corrosion resistance.

Keywords: magnesium alloy; Ca-P coating; electrodeposition; corrosion; DCPD

1. INTRODUCTION

Magnesium and its alloys have attracted much attention as a biodegradable implant material due to their good biocompatibility and biodegradability recent years [1,2]. Unlike traditional permanent implants, such as Ti alloys and stainless steels, biodegradable magnesium alloys will not cause permanent physical irritation or chronic inflammatory discomfort. [1,2] Additionally, the density and mechanical properties of magnesium-based alloys are close to those of nature bone [1,3]. The elastic modulus of magnesium alloys is about 45GPa and is much lower than those of stainless steels

(~200GPa), Co-Cr alloys (~230GPa), and Ti alloys (~110GPa). Magnesium alloys can dramatically reduce the stress shielding effect induced by serious differences between the elastic modulus of implants and nature bones. Therefore, magnesium alloys have potential biomedical applications as biodegradable biomaterials.

Magnesium and its alloys degrade in aqueous environments via an electrochemical reaction producing magnesium hydroxide and hydrogen gas [2]. Especially in vivo where the chloride content of the body fluid is about 150mmol/l (which has exceeded the critical concentration 30mmol/l), the degradation rate is faster due to the magnesium hydroxide converts into highly soluble magnesium chloride [4-6]. The rapid degradation rate of the magnesium-based implants in vivo has become the main limitation hindering their applications [7]. Suitable strategies are thus required to be developed to tailor their degradation rates.

To tailor the degradation rate of the Mg-based implant for the specific biomedical application, a lots of studies have been performed for the purpose of reducing the corrosion rate of Mg. Surface modification is an effective way to improve the biodegradation property as well as the biocompatibility of Mg alloys. [8-13] Calcium phosphates, the major composition of bone, have demonstrated high biocompatibility, osteoconductivity and non-toxicity in an in vivo environment.[12-16] Such evidence advocates that bioactive CaP coating on Mg alloys might be an effective way to solve this problem. Though many methods for fabricating CaP coatings are available, electrochemical deposition (ED) methods are widely used for coating calcium phosphates on metallic implants [17-19], due to their ease of operation and practicability for coating complex structures. Recently, ED methods have been applied for coating calcium phosphates on magnesium alloys [20-22]. However, there are no studies which investigate the effect of bath temperatures on the microstructure and corrosion properties of electrodeposited CaP coatings on magnesium alloys in the literatures.

For avoiding the fast degradation of pure Mg and improving the mechanical properties, 5.5 wt.% zinc and 0.5 wt.% Zr were picked up as the alloy elements in our biodegradable magnesium alloy. Zn²⁺ as a bivalent trace metal is centrally involved in electron acceptance, serving as coordinating points in human metabolism for the metalloproteins and enzymes [23]. As one of the most important essential tracer metals of human nutrition, its deficiency is a world nutritional problem [24]. Zinc is recognized as a highly essential element for humans. In zinc deficiency, nearly all the physiological functions are strongly perturbed. Zirconium possesses a set of suitable properties for orthopedic applications such as low specific weight, high corrosion resistance, and biocompatibility. Based on the above considerations, ZK60 magnesium alloy (Mg-5.5wt%Zn-0.5wt%Zr) was chosen in our studies.

In this study, CaP coatings were electrodeposited onto ZK60 magnesium alloy substrates at different electrolyte temperatures. The effects of electrolyte temperature on the microstructure, composition of the CaP coatings and the in vitro degradation properties of CaP coated ZK60 alloy were investigated, in order to optimize the fabricating procedure of CaP coatings on Magnesium alloys.

2. EXPERIMENTAL

2.1 Sample Pretreatment

The magnesium alloy used in this study was ZK60 alloy, with the major alloying elements of approximately 5.5wt% Zn and 0.5wt% Zr. It was cut into rectangular samples with a size of $10 \times 10 \times 5 \text{ mm}^3$. These samples were ground with SiC papers up to 800#, rinsed ultrasonically in ethanol and then air dried.

2.2 Electrodeposition

The experimental set up used for the electrodeposition was a simple two-electrode cell configuration. The working electrode was the ZK60 alloy and the counter electrode was a platinum sheet. Both electrodes were immersed in a supersaturated electrolyte (SE) which was prepared by dissolving given amounts of reagent-grade chemicals $\text{Ca}(\text{NO}_3)_2 \cdot 4\text{H}_2\text{O}$, $\text{NH}_4\text{H}_2\text{PO}_3$ and H_2O_2 , in demineralized water. The ion concentrations of electrolyte are listed in Table 1.

Table 1. Composition of electrolyte solution

Component	Concentration (/L)
$\text{Ca}(\text{NO}_3)_2 \cdot 4\text{H}_2\text{O}$	0.1 mol
$\text{NH}_4\text{H}_2\text{PO}_3$	0.06 mol
30% H_2O_2	15~20 mL

2.3 Surface Characterization

The crystallographic structure and chemical compositions of the coatings were examined using X-ray Diffraction (XRD) and energy dispersive spectroscopy (EDS), respectively. To study the morphology, coated samples were analyzed with a field emission scanning electron microscope (FE-SEM).

2.4 Electrochemical Measurements

Corrosion behavior of the samples was studied by electrochemical tests (Tafel Plot) with an electrochemical work station. The experiments were performed in the simulated body fluid (SBF) solution (listed in Ref.23) with a pH value of 7.4 at 37 °C. A three electrode set-up with a saturated calomel reference and a platinum counter electrode was used. The area of the samples for working electrode was $10 \times 10 \text{ mm}^2$. Prior to characterization, the samples were immersed in the solution for 20 min to establish the open circuit potential.

2.5 Immersion Tests

In vitro immersion tests were carried out in SBF solution. The pH value was adjusted to 7.4 ± 0.1 and the temperature was kept at 37 ± 0.5 °C using a water bath. The samples were immersed into 120 ml SBF solution for 8 days, respectively. The pH value of the solution and the samples' mass were recorded during the immersion every 24h, with a blank SBF solution as control group.

3. RESULTS AND DISCUSSION

3.1 Characterization of as-prepared CaP coatings

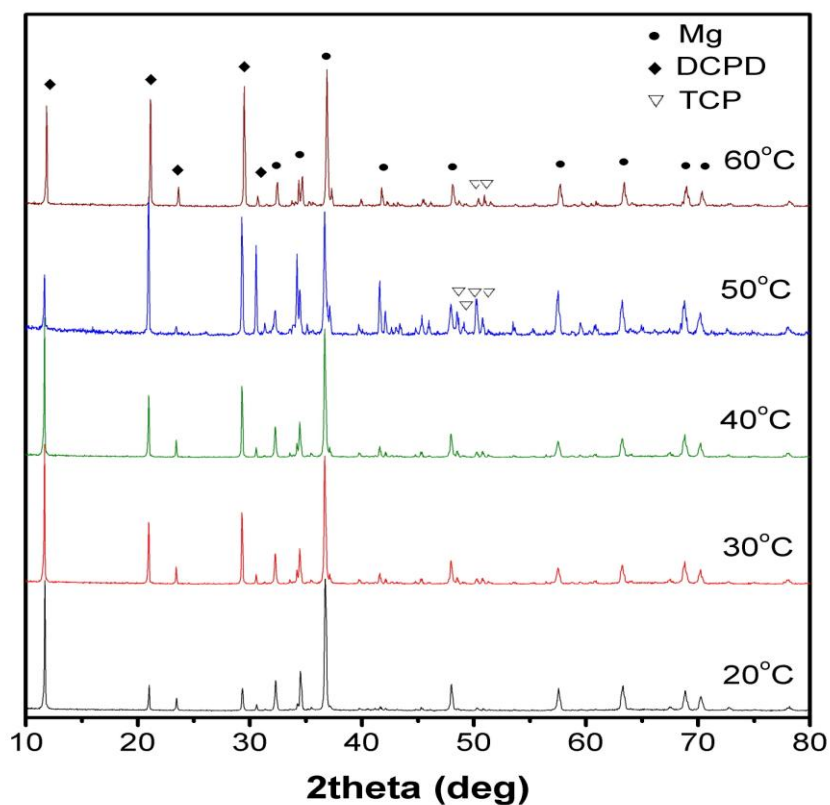
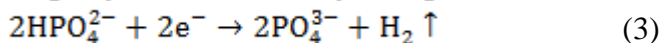
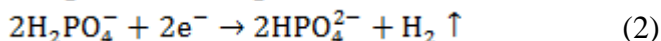
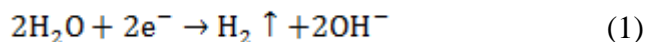


Figure 1. XRD patterns of ZK60 alloys with CaP coatings electrodeposited at different electrolyte temperatures

Fig.1 shows the XRD results of ZK60 alloys with CaP coatings electrodeposited at different electrolyte temperatures. The patterns show strong peaks at diffraction angle 2θ of 12° , 21° and 29° , which are typical diffraction peaks of DCPD ($\text{CaHPO}_4 \cdot 2\text{H}_2\text{O}$, PDF 72-1240). Also, weak peaks of β -TCP (tricalcium phosphate, $\text{Ca}_3(\text{PO}_4)_2$) are indexed in the XRD patterns. Thus, it can be clarified that the CaP coatings are composed of DCPD phase and a small amount of β -TCP phase. It can be seen that there is no significantly changes in the patterns of samples electrodeposited at different temperatures. But at high depositing temperatures, the peak intensities of β -TCP phase increase. This indicates that part of the DCPD phase transforms to β -TCP phase and the amount of β -TCP in the CaP coating increases with increasing depositing temperatures.

The cathode reactions of electrodeposition CaP phases on the surface of magnesium alloy are generally suggested as follows:

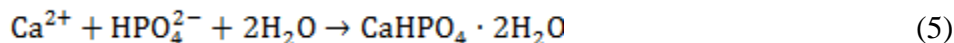


Supersaturated electrolytes buffered at pH 4 have been used for depositing CaP coatings. In the electrolyte, reactions (1) and (2) mainly occurred and generated HPO_4^{2-} would partially be deoxidized to PO_4^{3-} , as shown in reaction (3). Both hydrogen gas and hydroxyl ion were produced on the cathode surface. The deposition rate in electrochemical deposition is much higher than that in normal chemical deposition. The high deposition rate leads to high release rate of hydrogen gas. The absorption of hydrogen gas in the magnesium surface will hinder the nucleation and growth of CaP phase, and leads to a loose structure of the CaP coatings. In present electrochemical process, hydrogen peroxide was added in the electrolytes as a strong oxidizer and it reacts in cathode as following:



Reaction (4) occurs much easier than reaction (1) in thermodynamics. This will avoid the generation of hydrogen gas in some extent and generate necessary hydroxyl ion for the deposition of CaP phase.

During deposition, Ca^{2+} ion will precipitate with HPO_4^{2-} and PO_4^{3-} anions to form $\text{CaHPO}_4 \cdot 2\text{H}_2\text{O}$ (DCPD) and $\text{Ca}_3(\text{PO}_4)_2$ (β -TCP), respectively:



These reactions are considered to be the ones having a major effect on the formation of calcium phosphates because of their active role in controlling the pH and producing hydroxyl ions.

Figure.2 shows the surface morphology (SEM) and composition (EDS) of the electrodeposited CaP coatings at different bath temperatures. The left part of Fig.2 shows the surface morphology of coatings in low magnification. It can be seen that CaP coatings are uniformly distributed on the surface. With increasing electrolyte temperature, the coating becomes denser and the particles size of CaP coatings also increases. It was noticed that increasing the temperature affected the uniformity of the coatings. An increase in temperature facilitated both the transport of ion and the crystal growth of CaP crystals leading to more uniform and thicker coatings. We also can observe that the surface roughness increases with increasing electrolyte temperature.

The middle part of Fig.2 shows the surface morphology of coatings in high magnification. The coating surfaces exhibited two kinds of different crystal morphologies. One appeared regular flake-like structure diverging from centre toward periphery. The other appears irregular flake-like structure with different dimension. For the coating deposited at 20 °C, the CaP crystals are irregular flake-like structure. The flakes were about 2-5 μm in thickness and distributed randomly on the ZK60 substrate. When the deposition temperature is increased to 30 °C, a dendritic structure, composed of regular flakes which were about 2-5 μm in thickness and 50-100 μm in length, was observed in the coating. Further increasing the temperature to 40 °C, the flakes tend to aggregate and form several flower-like structure. At 50°C, the morphology of the coating is similar to that electrodeposited at 40 °C, but the flakes aggregate more closely.

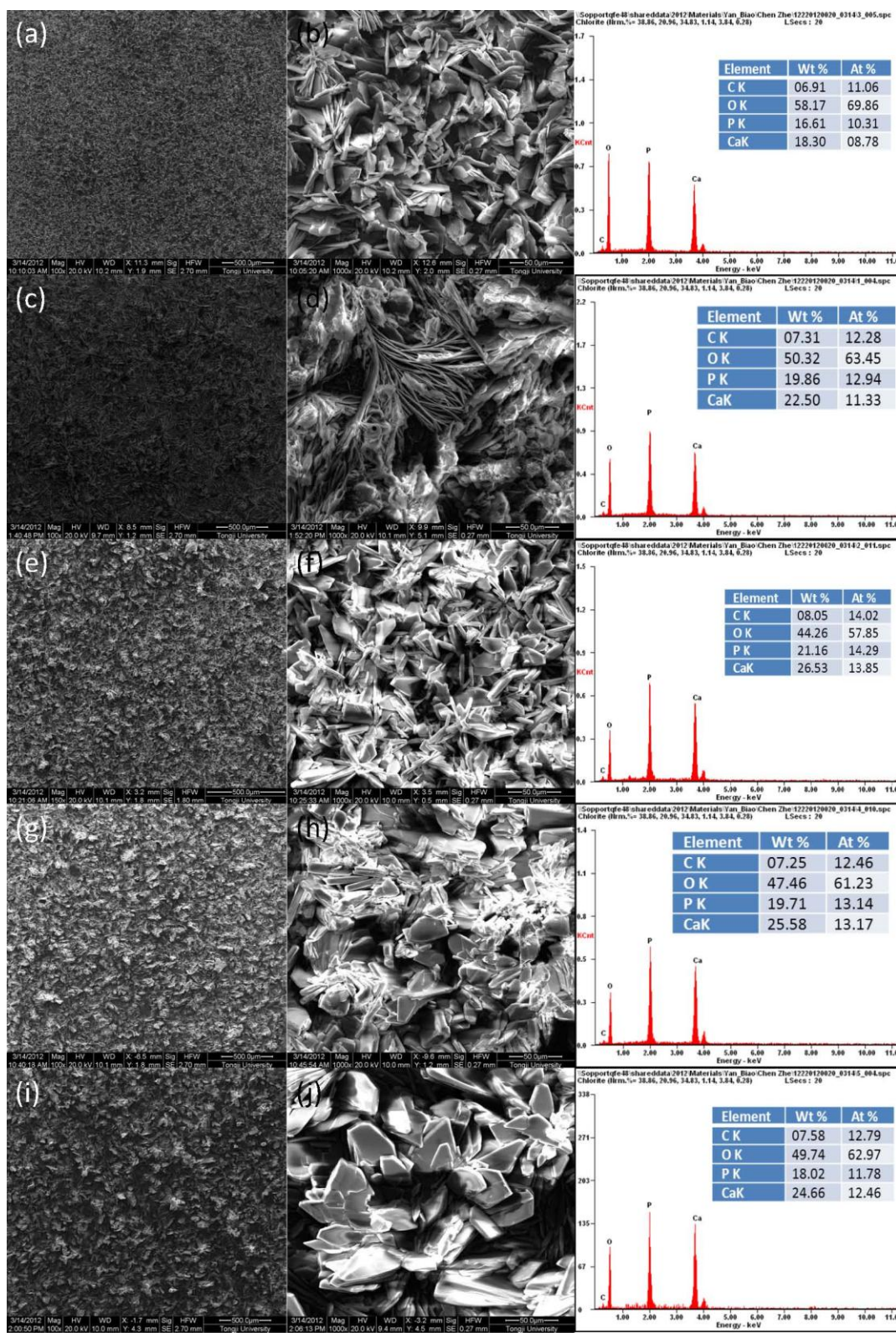


Figure 2. SEM morphologies and corresponding EDS patterns of coated samples. 20°C: (a)/(b); 30°C: (c)/(d); 40°C: (e)/(f); 50°C: (g)/(h); 60°C: (i)/(j)

When the the deposition temperature is up to 60 °C, we can clearly see that there are two layer in the coating. The first layer is composed of closely-packed flakes while the upper layer is composed of bigger irregular flakes.

The compositions of the coatings electrodeposited from the electrolyte solution at different temperature were examined by EDS, as shown in the right part of Fig.2. The main elements detected on the surface of the coatings were Ca, P, C, and O indicating that CaP phase was present in the coating. EDS analysis of the various coatings revealed that Ca/P atomic ratio was found to be around 0.851, 0.876, 0.969, 1.002 and 1.058 for coatings deposited at electrolyte temperature of 20 °C, 30 °C, 40 °C, 50 °C and 60 °C, respectively. The Ca/P ratios of all the coatings are close to that of the stoichiometric DCPD (1). This result indicates that our DCPD coating is calcium-deficient at low electrolyte temperature (less than 40°C). This is due to substitutions in the lattice. Calcium phosphate compounds can be substituted with different ions. In the DCPD lattice, calcium can be replaced by small amounts of magnesium and sodium, and phosphates can be replaced by carbonate ions [19]. During the electrodepositing process, these ions are incorporated into the coating. It is also known that there may be a significant amount of magnesium incorporated into coatings which makes calcium magnesium brushite the mostly like phase present due to the corrosion of the substrate during the coating process. Substitution and interstitial Mg in the lattice affect the growth of the CaP crystal structure [25, 26]. With increasing electrolyte temperature, the Ca/P atomic ratio in the coatings increases. The increase Ca/P atomic ratio mainly results from the formation of β -TCP phase, which has a stoichiometric Ca/P ratio of 1.5. XRD results confirm that there is a small amount of β -TCP phase in the CaP coatings electrodeposited at high temperatures.

3.2 Electrochemical test in SBF

The potential dynamic polarization curves (PDP curves) obtained for CaP-coated and uncoated ZK60 alloy samples in SBF solution at 37 °C were plotted based on the electrochemical characterizations, as shown in Fig.3. Generally, the cathodic polarization curves are assumed to represent the cathodic hydrogen evolution through water reduction, while the anodic ones represent the dissolution of magnesium. The cathodic parts of the curves in Fig. 3 indicate that the cathodic polarization current of the hydrogen evolution reaction on the DCPD-coated Mg alloy is much higher than that on the uncoated Mg substrate. That is to say, the overpotential of the cathodic hydrogen evolution reaction is lower on the DCPD-coated Mg alloy than on the uncoated Mg substrate. This also reveals that the cathodic reaction is easier kinetically on the DCPD-coated specimen than on the bare one, which may be due to the existence of the DCPD coating. Tafel-type analysis was performed on the linear regions of the plot, using the Tafel slopes from between 50 and 250mV away from the corrosion potential, to provide an approximation of the corrosion current density. Values of the corrosion potential E_{corr} and the corrosion current density i_{corr} were extracted from these curves and are shown in Table 2. It is known that a material that has a higher corrosion potential will have a lower degradation rate. The initial corrosion potential (E_{corr}) of the DCPD-coated Mg alloy samples were all higher than the uncoated alloy sample (-1.53V) and increase from 1.42 V to 1.33 V with increasing

electrolyte temperatures (20-60 °C), as shown in Table 2. While the corrosion current density I_{corr} is about 2-3 order of magnitude lower than that of the uncoated magnesium. This result further indicates that the corrosion resistance of magnesium has been improved by the DCPD coating. The lower corrosion current density was due to the smaller portion of exposed area to the solution. Thus, there was a decrease in anodic reaction rate (the corrosion rate). The coating decreases the available surface area susceptible to corrosion. The corrosive solution cannot attack the magnesium where it is protected by the CaP coating. This matched with the immersion testing results that the initial degradation rate of the CaP-coated samples was lower than the uncoated ones. In all the samples, the sample coated at 60 °C has the best in vitro corrosion resistance. This is because that the higher electrolyte temperature will lead to thicker and denser coatings. From the results of electrochemical testing analysis, it is obvious that the Ca-P coating could improve effectively corrosion resistance of the ZK60 alloy in the SBF solution. The improvement in corrosion resistance will greatly reduce the initial biodegradation rate of the implants, and is essential for maintaining the implant's mechanical strength in the bone reunion period. In terms of the design of degradable implants, this means that a thinner or less bulky bone plate could be used compared with untreated Mg implants having the same service life.

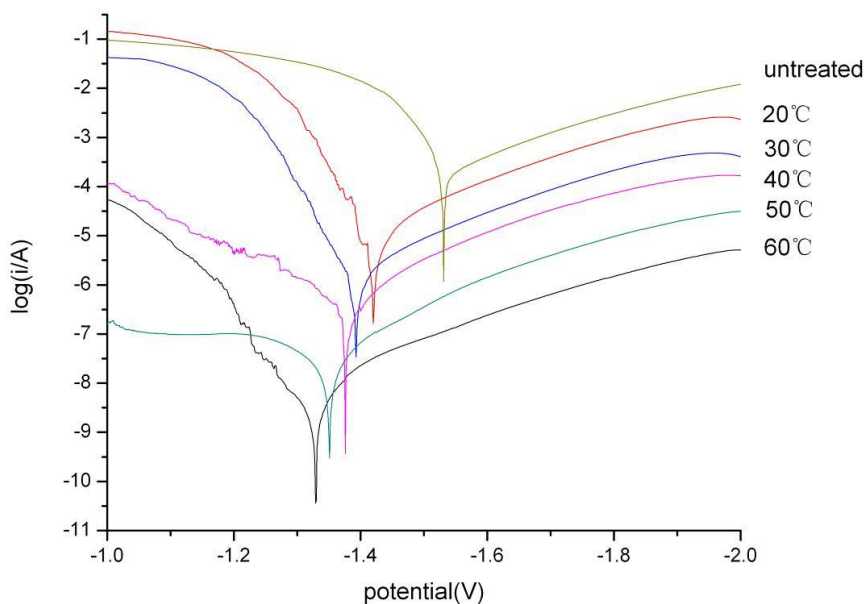


Figure 3. Tafel plot of the samples in SBF solution

Table 2. Corrosion parameters obtained from electrochemical analysis

samples	E_{corr} (V)	I_{corr} (A)
uncoated	-1.531	1.768e-004
20°C	-1.420	6.258e-007
30°C	-1.393	3.466e-007
40°C	-1.376	1.664e-006
50°C	-1.351	4.145e-006
60°C	-1.329	3.391e-007

3.3 In vitro immersion test

To examine the long-term corrosion behavior, the in vitro corrosion behavior of the CaP-coated and uncoated ZK60 alloy samples in SBF were monitored. The pH values of the SBF were monitored every day during the sample immersion. Fig.4 shows the variation of the pH value of SBF solution at different immersion time. The corrosion rate of Mg alloys during the early stages of implantation would play a critical role in the initial surrounding tissue response. If the initial degradation of Mg-based implants was too rapid, osteolysis would occur, thus adversely affecting bone tissue regeneration.[27] Therefore, it was critical to control and decrease the initial degradation rate. From Fig.4, it can be seen that there is an increase in pH value for all the samples with increasing time. At the first day, the pH value increases sharply for all the samples because of the increase of OH⁻ concentration caused by the release of Mg²⁺ [28]. The pH for the uncoated sample increases from 7.4 to 8.5 while the pH of coated samples increase only about 0.4 (reach to 7.8) (The relatively lower increases in pH in current study compared to previous studies [10-13] are because that only one surface of the samples is exposed to the SBF solution). After 2 days' immersion, the pH changes for all samples slow down. It is clear that the pH change for the uncoated sample was the highest and the pH value reaches to about 10 while the pH values of the solution immersed with CaP coated samples are around 8.4, which is much lower than that of uncoated samples. Comparing with other samples, the samples electrodeposited at 50 and 60 °C have the smallest pH change and thus best corrosion resistance. Therefore, it can be concluded that the samples coated with CaP have a better corrosion resistance than uncoated sample.

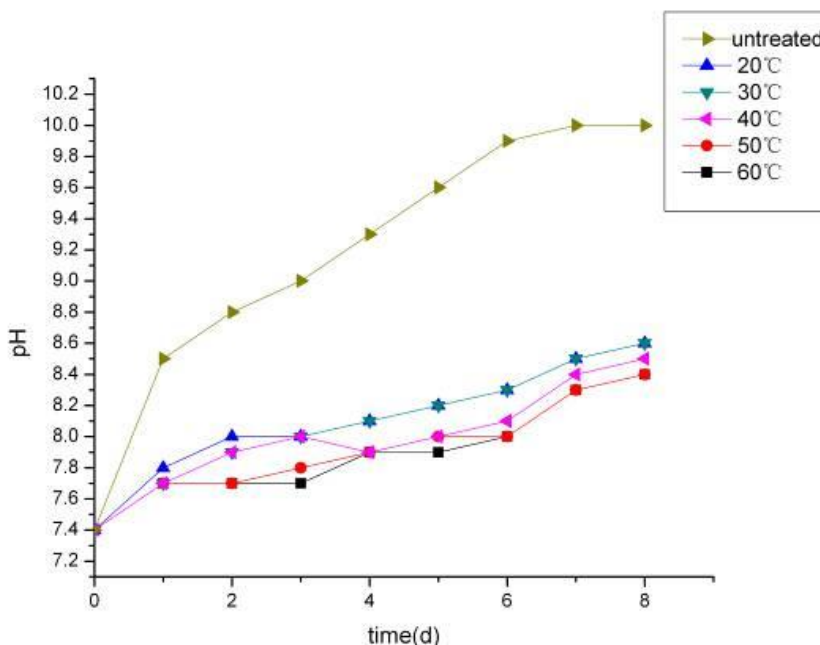


Figure 4. Variation of the pH value of SBF solution at different immersion time

Fig.5 shows the relationship of sample weight versus immersion time. It was observed that the weight of coated samples do not change much and keep almost constant (there are a little bit increase) with increasing immersion time while that of uncoated sample decreases significantly. The weight

change of the samples immersed in SBF solution was a result of the following three processes: (1) the corrosion of magnesium, (2) the precipitation of CaP coating, and (3) the dissolution of CaP coating.

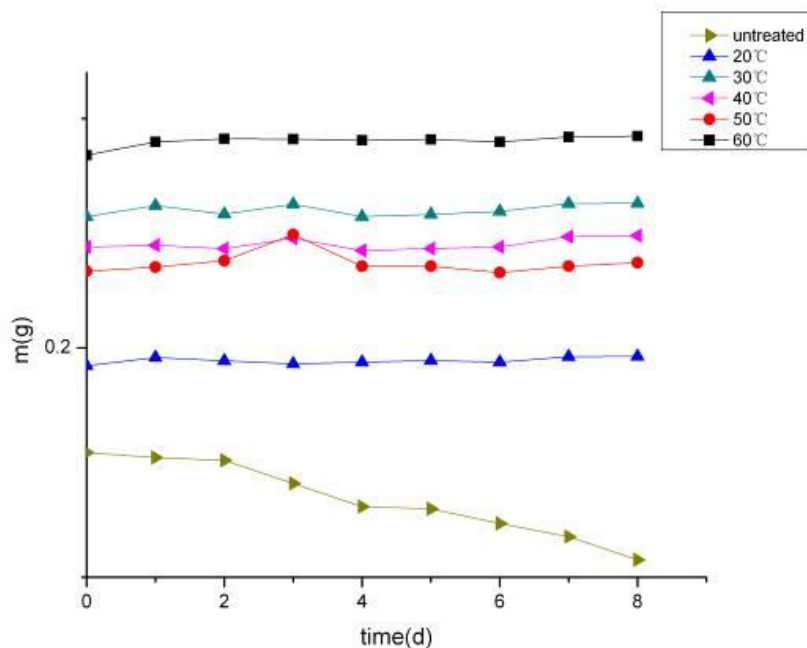


Figure 5. Relationship of sample weight versus immersion time

The corrosion of magnesium occurred for all the samples, but their corrosion rates were significantly different owing to varied surface coatings applied to the substrate, including no coating and coating at different electrolyte temperatures. Besides the corrosion of magnesium, CaP precipitation and dissolution were two processes continuously occurred during the immersion in SBF solution. As the CaP coating was mainly DCPD phase (DCPD has better solubility than other CaP phases), it could dissolve in a physiological solution at a body temperature. It can be proposed that the CaP coating underwent a dynamic process of precipitation and dissolution during the immersion test. For the samples with CaP coatings, there was a small increase in the weight of the samples after immersion in SBF solution for 8 days. This indicates that more CaP phase was formed during the soaking in SBF solution, where the CaP precipitation process predominated over the dissolution process.

4. CONCLUSIONS

In summary, CaP coating was successfully prepared on the ZK60 magnesium by electrodeposition. The CaP coatings show a DCPD phase structure with small amount of β -TCP phase and the Ca/P ratio is in the range of 0.85~1.06. The surface morphology shows a flake-like structure. The particle size and surface roughness in the coatings increase with increasing electrolyte temperatures. The Ca-P coating has tailored the corrosion of the magnesium substrate. The corrosion resistance of ZK60 alloy is obviously improved after coated with DCPD coatings and the sample with CaP coating deposited at 60 °C has the best corrosion resistance. The improvement in corrosion

resistance will greatly reduce the initial biodegradation rate of the implants, and is essential for maintaining the implant's mechanical strength in the bone reunion period. Thus ZK60 alloy coated with the Ca-P coating prepared in this study is a promising candidate for biodegradable orthopedic implant.

ACKNOWLEDGEMENTS

The present work was supported by National Natural Science Foundation of China (Grant No. 51071109) and Natural Science Foundation of Shanghai (Grant No. 13ZR1443700).

References

1. Mark P. Staiger, Alexis M. Pietak, Jerawala Huadmai, George Dias. *Biomaterials*, 27 (2006) 1728–1734
2. Frank Witte, Norbert Hort, Carla Vogt, Smadar Cohen, Karl Ulrich Kainer, Regine Willumeit, Frank Feyerabend. *Curr. Opin. Solid State Mat. Sci.*, 12 (2008) 63–72
3. A. Feng, Y. Han, *J. Alloy. Compd.*, 504 (2010) 585–593
4. B.A. Shaw. Corrosion resistance of magnesium alloys. In: Stephen D, editor. ASM handbook volume 13a: corrosion: fundamentals, testing and protection. UK: ASM International; 2003.
5. F. Witte, V. Kaese, H. Haferkamp, E. Switzer, A. Meyer-Lindenberg, C.J. Wirth, et al. *Biomaterials*, 26(2005) 3557–3563.
6. F. Witte, J. Fischer, J. Nellesen, H.A. Crostack, V. Kaese, A. Pisch, et al. *Biomaterials* 27(2006) 1013–1018.
7. F. Witte. *Acta Biomaterialia*, 6 (2010) 1680–1692.
8. Li KaiKai, Wang Bing, Yan Biao, Lu Wei. *J. Biomater. Appl.*, doi: 10.1177/0885328212453958
9. Jingxin Yang, Fuzhai Cui, and In Seop Lee. *Annals of Biomedical Engineering*, 39, (2011) 1857–1871
10. Li KaiKai, Wang Bing, Chai Jing, Yan Biao & Lu Wei. *Sci. China Tech. Sci.*, 56 (2013) 80-83
11. Wei Lu, Zhe Chen, Ping Huang and Biao Yan. *Int. J. Electrochem. Sci.*, 8 (2013) 9518 - 9530
12. Wei Lu, Zhe Chen, Ping Huang and Biao Yan. *Int. J. Electrochem. Sci.*, 7 (2012) 12668 - 12679
13. Li KaiKai, Wang Bing, Yan Biao & Lu Wei. *Chin. Sci. Bull.*, 57 (2012) 2319-2322
14. Pamela Habibovic, Florence Barre`re, Clemens A. van Blitterswijk, Klaas de Groot, and Pierre Layrolle. *J. Am. Ceram. Soc.*, 85 (2002) 517–22
15. Tal Reiner, Leonid M. Klinger, and Irena Gotman. *Crystal Growth & Design*, 11 (2011) 190–195
16. Shaylin Shadanbaz , George J. Dias. *Acta Biomaterialia*, 8 (2012) 20–30
17. M.C. Kuo, S.K. Yen. *Mater. Sci. Eng. C*, 20 (2002) 153–160
18. M. Ma, W. Ye, X.-X. Wang. *Mater. Lett.*, 62 (2008) 3875–3877
19. D.J. Blackwood, K.H.W. Seah. *Mater. Sci. Eng. C*, 29 (2009) 1233–1238
20. E.C. Meng, S.K. Guan, H.X. Wang, L.G. Wang, S.J. Zhu, J.H. Hu, C.X. Ren, J.H. Gao, Y.S. Feng. *Applied Surface Science*, 257 (2011) 4811–4816
21. M. Bobby Kannan. *Materials Letters*, 76 (2012) 109–112
22. M. Bobby Kannan, O. Wallipa. *Materials Science and Engineering C*, 33 (2013) 675–679
23. P. Jacobs, L. Wood. *Dm: Dis. Mon.*, 49 (2003) 601–608
24. M.J. Salgueiro, M. Zubillaga, A. Lysionek, M.I. Sarabia, R. Caro, T. De Paoli, A. Hager, R. Weill, J. Boccio. *Nutr. Res.*, 20 (2000) 737–755
25. F. Barrere, *Biomimetic Calcium Phosphate Coatings: Physicochemistry and Biological Activity* , University of Twente, Enschede, 2002
26. A. Bigi, G. Falini, E. Foresti, A. Ripamonti, M. Gazzano, N. Roveri, *J. Inorg. Biochem.*, 49 (1993)

69–78.

27. R. G. Guan, I. Johnson, T. Cui, T. Zhao, Z. Y. Zhao, X. Li, H. Liu, *J. Biomed Mater Res A.*, 100 (2012) 999-1015

28. A. Atrens, M. Liu, N. I. Z. I. Abidin, *Mater. Sci. Eng. B*, 176 (2011) 1609-1636

© 2013 by ESG (www.electrochemsci.org)